NUMERICAL SIMULATION OF MICROCELLULAR INJECTION MOLDING: A CASE STUDY

A. Chaabene, A. Ben Khalifa, S. Chatti*

Laboratory of Mechanical Engineering (LGM), National Engineering School of Monastir, University of Monastir, Rue Ibn El Jazzar, 5000 Monastir, Tunisia
*Corresponding author's e-mail address: sami.chatti@udo.edu

ABSTRACT

The microcellular injection molding, often referred to as MuCell®, is an innovative polymer processing technique that utilizes supercritical inert gases, such as CO_2 or N_2, to manufacture lightweight plastic products. This technology has gained significant attention in recent years due to environmental concerns and the increasing demand for lightweight components with superior mechanical properties. However, challenges related to surface finish quality and limited mechanical properties have impeded its widespread adoption. This paper provides a comprehensive overview of the microcellular injection molding process. To evaluate the practicality of the MuCell® process, an industrial case study is conducted, assessing its production reliability and overall product quality. A comparative rheological analysis is performed to discern the distinctions between MuCell® and traditional injection molding, thus validating the claimed advantages of microcellular injection. Based on the accrued findings, it is deduced that MuCell® proves to be a pertinent injection molding technique for fabricating lightweight plastic components featuring enhanced dimensional stability, reduced shrinkage, and minimized warping when compared to conventionally injection-molded parts.

KEYWORDS: Plastic injection, microcellular injection molding, MuCell, mechanical properties, surface quality

1. INTRODUCTION

Plastic injection molding is a well-established replication process for cost-effective manufacturing of polymer-based components. This process finds diverse applications in fields such as medical, automotive, and aerospace industries.

The growing demand for lightweight and cost-efficient plastic components is driving chemists to explore advanced technologies, including the development of microcellular materials that offer additional functionalities.

Indeed, the Microcellular injection molding process, known as MuCell®, involves injecting a supercritical gas into the molten polymer and allowing it to expand and fill the tool cavity, creating a cellular structure within the part. Consequently, this results in lighter components with improved dimensional stability. Moreover, additional benefits are attainable through this process, including cost reduction due to material savings and reduced cycle times.

However, the adoption of MuCell® technology for automotive parts has not been widespread due to several factors, notably the high initial investment required for process implementation.

This article presents empirical evidence of the effectiveness of MuCell injection technology. To provide a tangible context for the study, an existing industrial example, a carrier side flank of a car, was selected to emphasize MuCell's capabilities and advantages in enhancing traditional production methods.

The primary aim of this study is to verify the profitability and reliability of the MuCell process concerning production and quality. The next section will provide a comprehensive review of the current state-of-the-art in this field. Section 3 will extensively delve into the rheological examination of the carrier side flank component, aiming at the substantiation of the properties asserted through MuCell injection simulations using the leading true-3D molding simulation software Moldex3D Plastic Molding, and engage in a thorough discourse on the outcomes. In section 4, a comprehensive comparative analysis between conventional injection and MuCell injection will be presented.

The article draws to a close with a comprehensive concluding section wherein we delineate the prospects of the project.

© *Galati University Press, 2024*

Date of submission/acceptance: 31.05.2024/15.12.2024 http://doi.org/10.35219/awet.2024.01

2. LITERATURE REVIEW

2.1. The Injection Moulding Process

An injection moulding system comprises several essential components, including the injection unit, mould closing unit, ejection unit, core pulling unit, and cooling unit. The primary objective of the injection unit is to transform the raw plastic material into a molten state and then inject it into the mould cavity. The critical components of the injection unit encompass a screw situated within a screw chamber, heating elements positioned around the screw chamber, and a hopper containing the plastic resin. These elements work in tandem to facilitate the plastic material's melting process, thereby reducing its viscosity, and enhancing its fluidity. As the screw advances within the screw chamber, it propels the molten polymer into the mould cavity, leading to increased material density and reduced shrinkage. Consequently, the injection molding cycle can be succinctly summarized as follows [1,2]:

- Plastic Injection: This initial phase of the injection moulding process involves the injection unit, where the raw plastic material is melted and injected into the mould cavity.
- Holding and Packing: Following the injection of the molten plastic into the mould, the holding and packing stage ensues. This step involves maintaining pressure on the material within the mould to ensure it fills all cavities completely and packing it tightly to minimize any voids or defects.
- Cooling and Solidification: Once the mould is filled and the plastic part is shaped according to the desired design, the cooling and solidification stage commences. During this period, the mould cools, allowing the molten plastic to solidify and take on its final form.
- Mold Opening and Part Ejection: Finally, in the last phase of the injection moulding process, the mould opens, and the newly formed plastic part is ejected from the mould cavity, completing the manufacturing cycle.

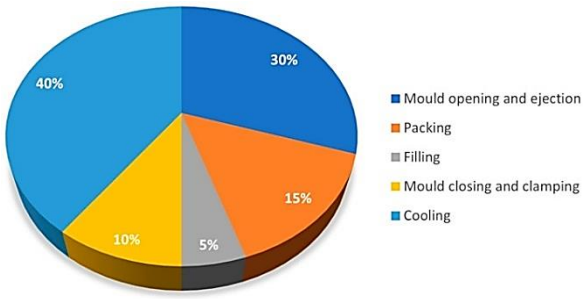

Fig. 1. Cycle time in injection moulding [3]

In figure 1, the representation displays the average percentage of each phase throughout the entire injection moulding cycle, as outlined in reference [3].

The total cycle duration is influenced by various factors, with the part wall thickness being particularly significant. However, it's worth noting that the cooling stage consistently consumes the most time, accounting for over half of the entire injection moulding cycle.

2.2. Motivation for the MuCell® Process

The automotive sector is a vital market for injection-moulded parts, particularly within the European Union (EU). This industry operates under stringent safety and environmental regulations. The EU's strict emissions restrictions have not only spurred the advancement of new energy-powered vehicles, including hybrids and electric cars but have also driven the development of more efficient and lightweight gasoline-powered vehicles. Consequently, the automotive industry now demands high-performance and lightweight plastic components more than ever before. This presents a substantial challenge for injection moulding companies that supply plastic parts to the automotive sector. They must embark on a process of redesigning existing injection-moulded components and developing innovative injection moulding strategies to meet the evolving demands of the industry.

Substituting solid injection-moulded parts with foamed ones offers an effective strategy for reducing the weight of components, as highlighted in references [4–5]. Thermoplastic foam parts can be manufactured using two primary types of blowing agents: chemical and physical blowing agents, as discussed in references [6,7,8]. In the case of chemical blowing agents, these agents are blended with the polymeric materials within the hopper and subsequently introduced into the barrel. As the temperature within the barrel reaches a specific threshold, gases such as nitrogen, carbon dioxide, or carbon monoxide are released. This release leads to the formation of an internal microcellular structure within the material, creating foam [9,10].

However, it's important to note that the use of chemical blowing agents does come with certain drawbacks. These include the potential for uneven bubble formation and the challenges associated with managing the residual chemical by-products within the injection moulding machine.

Microcellular injection moulding represents a foaming technology that utilizes a physical blowing agent, and one of the most recognized techniques in this field is MuCell® [6,11]. Nevertheless, recent developments have introduced other commercialized technologies, including Optifoam®, ProFoam®, Ergocell®, and IQ Foam®. Each of these technologies is grounded in the incorporation of a gas or supercritical fluid (SCF) into the melt during the injection moulding process, although they employ distinct methods for achieving this mixture [6,11,12,13].

In the MuCell® process, a specially designed reciprocating screw serves as the SCF dosing component. This elongated screw, unlike conventional

ones, is equipped with a mixing section designed to optimize the blending of the SCF with the polymer melt. Meanwhile, the Optifoam® process employs a specially designed nozzle as the SCF dosing apparatus. In the ProFoam® process, gas is introduced directly into the hopper and subsequently dissolves within the melt within the injection unit. In contrast, the Ergocell® process utilizes a dynamic mixer to blend the SCF with the melt. Lastly, the IQ Foam® process incorporates a two-chambered unit positioned between the hopper and the screw chamber to facilitate the mixing of the melt and gas at moderate-low pressures [6,11,12,13].

Among these various technologies, MuCell® has gained the most extensive industrial acceptance and holds a leading position in the field. Notably, these technologies, with MuCell® at the forefront, enable the production of lightweight plastic components while also contributing to a reduction in carbon footprint and CO2 emissions [14].

2.3. The MuCell® Process

The MuCell® microcellular injection moulding process originated at MIT (Massachusetts Institute of Technology, Cambridge, MA, USA) with the primary objective of reducing both the weight and production costs associated with plastic components [15]. This innovative process achieves a notable material reduction of approximately 30% to 40% while producing parts with enhanced impact strength and an internal structure characterized by a high density of small bubbles measuring 2 to 10 μm in size [15,16,17]. Moreover, the inclusion of a supercritical fluid in the polymer melt within the barrel also leads to a reduction in the melt's viscosity [18,19].

Initially, the microcellular foaming was executed through a batch process, resulting in extended cycle times and relatively large, foamed bubbles. Subsequently, Trexel (Wilmington, MA, USA) enhanced this technology by integrating it with an injection moulding machine, thereby creating a continuous process known as MuCell® Moulding [20].

The structure of a typical MuCell® machine, as illustrated in figure 2, comprises several key components, including an inert gas pump, SCF (Supercritical Fluid) metering system, SCF injector, front and back non-return valves, and a shut-off nozzle [21,22]. Within the SCF metering system, a mass flow element is responsible for regulating the level of SCF mixed with the molten polymer. The shut-off nozzle serves the crucial function of preventing the molten material from flowing back through the nozzle [20,23].

The primary MuCell® process can be distilled into four key steps [11,23,24,25,26]: SCF mixing and dissolution in the polymer melt, cell nucleation, cell growth, and solidification. In the gas dissolution step, an inert gas is pressurized to reach a supercritical fluid state and is then passed through the mass flow element to combine with the molten polymer within the screw chamber, located between the front and back non-return valves. The achievement of the supercritical fluid phase is accomplished by injecting the gas above its critical pressure (Pc) and critical temperature (Tc), as depicted in figure 3. The mixing of the supercritical fluid under pressure enhances its solubility within the polymer melt [27]. Typically, commonly used inert gases include carbon dioxide, known for its high solubility, and nitrogen, which permits a higher degree of foaming [10]. While other gases like argon and helium have been explored, they tend to be more expensive, flammable, and may lead to machine degradation [6].

Cell nucleation commences as the mixture of the supercritical fluid and the melt is injected into the mold cavity, triggered by a rapid pressure drop [10,11,13,21,28,29,30]. These cells continue to expand and enlarge as the mixture continues to be injected into the mould cavity, while the gas-polymer melt maintains an elevated temperature. Finally, in the last step, cell growth is arrested due to the cooling effect, leading to the solidification of the plastic part, which is subsequently ejected from the mould cavity.

Cell nucleation in microcellular injection moulding involves two primary mechanisms: homogeneous and heterogeneous nucleation [17,30]. Here's a breakdown of these mechanisms and related findings:

Homogeneous Nucleation: This occurs when gas dissolved into a homogeneous polymer melt without any impurities or additives. It's a process where bubbles form within the polymer melt itself, and it typically results in a smaller number of larger bubbles.

Heterogeneous Nucleation: In contrast, heterogeneous nucleation occurs when bubbles form at interfaces between two different phases, such as the polymer and an additive. In this case, nucleation occurs on the surface between the additives or fillers and the SCF-polymer melt. Heterogeneous nucleation generally occurs more rapidly than homogeneous nucleation due to its lower activation energy. It often leads to a larger number of smaller bubbles.

Additives are commonly used in polymers, which may prevent the formation of a homogeneous mixture and result in a smaller number of larger bubbles. To generate a higher number of smaller bubbles, additives must be introduced into the polymer [33,34,35].

Bubble Size and Mechanical Properties: Research by Moon et al. [36] using polypropylene (PP) demonstrated that smaller bubble sizes contribute to better mechanical properties in microcellular parts. Increasing gas saturation pressure was found to increase bubble density, decrease the energy barrier for nucleating stable bubbles, and reduce bubble diameter. The gas saturation pressure was also observed to limit bubble growth within very short timeframes. However, there were some differences between experimental results and theoretical models due to simplifications in the theoretical approach.

Cell Structure: Dong et al. [37], using acrylonitrile butadiene styrene (ABS), investigated the cell structure of microcellular injection-moulded parts along both the vertical and parallel directions to melt flow. They found the presence of both round and distorted cells in the moulded part. These two cell shapes were attributed to different stages of MuCell® process. Distorted cells were formed during the filling stage, influenced by the fountain-flow effect, while round cells were created in the cooling stage due to cooling-induced shrinkage.

Effect of Additives in Semi-Crystalline Polymers: Colton et al. [31] studied the microcellular foaming process in semi-crystalline polypropylene and the impact of various additives. Unlike amorphous materials, semi-crystalline polymers have long chains arranged uniformly and crystalline areas that limit gas dissolving space and may physically impede the foaming process. However, the nucleation mechanism in semi-crystalline polymers was found to be like that in amorphous polymers.

Influence of Shot Size: Behravesh and Rajabpour [22,39] explored cell formation in the filling stage using high-impact polystyrene. They determined that shot size played a dominant role in cell formation and growth. A smaller shot size resulted in higher foam percentages but incomplete cavity filling. Conversely, a larger shot size filled the mould cavity completely but resulted in lower foaming values or no foaming.

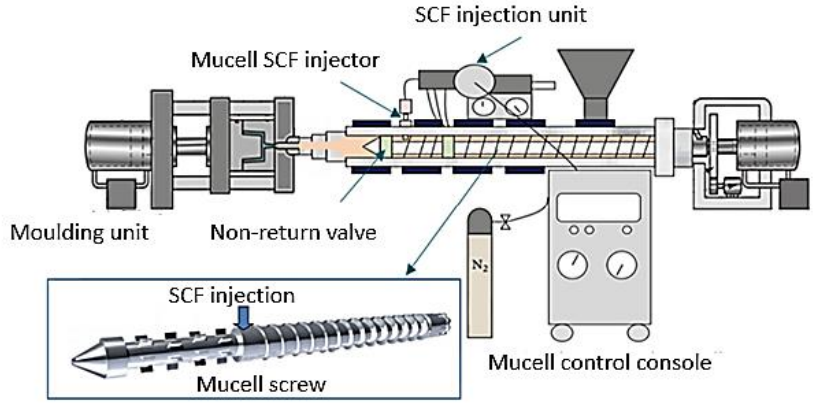

Fig. 2. Diagram of the MuCell injection system [13]

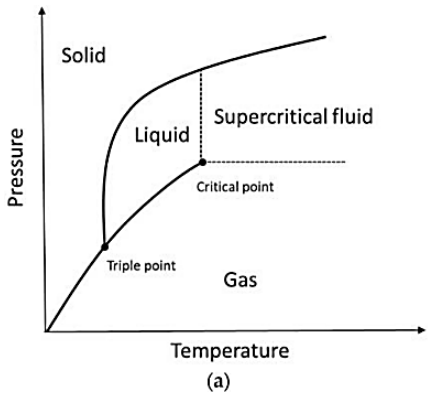

	Tc	Pc
N_2	−147 °C	34 bar
CO_2	31 °C	71 bar

(b)

Fig. 3. a) Definition of a supercritical fluid status;
b) Critical temperature (Tc) and critical pressure (Pc) of N_2 and CO_2 [17]

Core-Back Process: Several authors [28,40,41] highlighted the core-back process as a facilitator of the nucleation process. It involves retracting the moving part of the mould after cavity filling, creating a rapid pressure drop and allowing a time delay for the solid skin to form. This process enables high cell fractions, reducing weight and improving stiffness-to-weight ratios.

In conclusion, microcellular injection technology is an innovative approach to injection moulding that leverages the inclusion of gas bubbles within plastic parts to achieve improved mechanical properties, reduced weight, enhanced thermal insulation, and other unique characteristics. Its applications span various industries, contributing to the development of lightweight, high-performance products.

2.4. Comparison between Micro-Cellular Injection Moulding and Standard Injection Moulding

Certainly, here is a recapitulatory comparison between microcellular injection moulding and standard injection moulding presented in Table 1.

In summary, microcellular injection moulding offers benefits such as reduced weight, improved mechanical properties, and thermal insulation compared to standard injection moulding. However, it comes with increased complexity and potential cost implications. The choice between the two methods depends on the specific requirements of the intended application and the desired balance between material properties, cost, and process complexity.

In our study, we will assess and compare the features presented by the MuCell® process with those of conventional injection moulding and show, based on an industrial case, the technical differences.

3. RHEOLOGICAL STUDY OF MICRO-CELLULAR INJECTION MOULDING

The manufacturing of upper right and left side panels for the carrier side flank of a car using Microcellular injection technology at a plastic injection company should be analyzed in our study. The aim is to verify the profitability of the MuCell process and its reliability in terms of production and quality and to improve its prospects and opportunities.

For optimal results, precise calculations are imperative in plastic injection moulding. This underscores the crucial role of rheology in plastics processing, as it empowers us to anticipate the merits and drawbacks of a geometric model (as presented in a CAD (Computer Aided Design) file) as it undergoes transformation into a finite element mesh.

Within this section, we will conduct a comprehensive rheological analysis on the carrier side flank component. The objective is to facilitate a comparative evaluation between conventional injection moulding and microcellular injection moulding techniques.

Before starting the rheological study, it is important to check that the part has been thickened, i.e., that it has been properly assembled and closed to be filled. So, the methodology to follow is to go from a surface body to a volume body using SolidWorks software (Fig. 4).

Table 1. Comparison between microcellular injection moulding and standard injection moulding

Aspect	Microcellular Injection Moulding	Standard Injection Moulding
Cellular Structure	Foam-like microcellular structure	Homogeneous, solid structure
Density and Weight	Lower density, lighter-weight parts	Higher density, heavier parts
Mechanical Properties	Improved stiffness, impact resistance	Consistent mechanical properties
Material Consumption	Less material consumption, cost savings	More material consumption
Thermal Insulation	Effective thermal insulation	Limited inherent insulation
Surface Finish	Smoother and more uniform surfaces	Variable surface finish
Complexity of Process	Additional complexity due to gas injection	Simpler process
Applications	Lightweight, improved properties	Wide range of plastic parts
Cost Considerations	Higher equipment and operational costs	Potentially lower initial costs

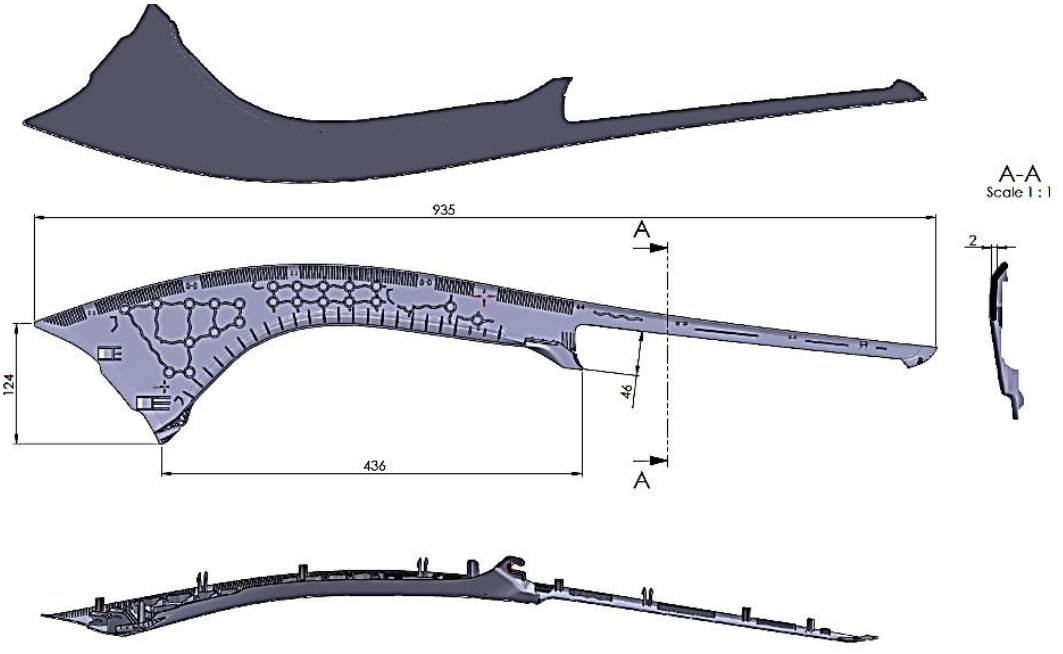

Fig. 4. Solid body of the component

3.1. Choice of Threshold Type and Position

Ensuring a continuous flow of material is crucial to obtain a defect-free gate. To achieve this, the direct injection method is employed. This approach involves the direct delivery of molten material into the mould cavity without any intermediaries, facilitating a uniform, uninterrupted flow. By eliminating unnecessary detours or interruptions in the injection path, direct injection minimizes the likelihood of injection-related defects, contributing to the production of high-quality components with consistent properties. For this design, the injection lug illustrated in figure 5 has been employed as a support structure for the gates. Three circular weirs with a diameter of 4mm have been used, as shown in figure 5.

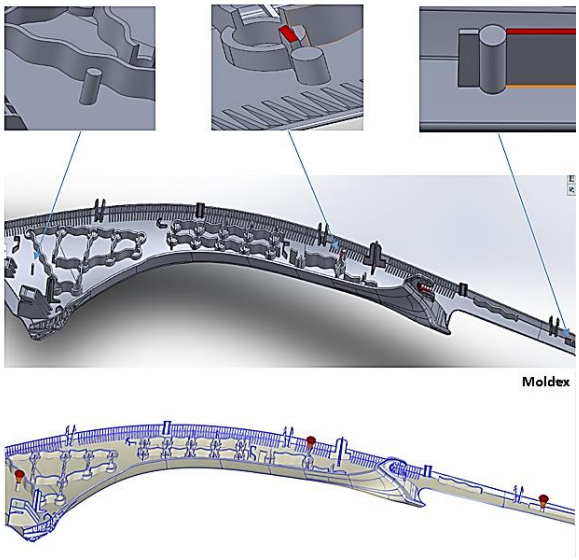

Fig. 5. Injection gate design

3.2. Meshing

To perform a finite element simulation, the component model must be meshed, which involves creating a set of nodes and elements. The choice of mesh depends on several parameters, including size, type (tetrahedral, hexahedral, or hybrid), and quantity. In our specific case study, the component is of substantial size; hence, we opt for a larger mesh size to accommodate the various intricacies of the part. Firstly, we have established the mesh using the tools provided by Moldex3D. After fixation, we locally refined the injection point area (Fig. 6).

Ensuring accurate and dependable results hinges on maintaining a high-quality mesh. The quality of a mesh is typically evaluated using an aspect ratio, which provides insights into the mesh's effectiveness. To uphold the precision of our simulations, it is imperative to sustain an aspect ratio consistently below 0.01 across all points on the component. This criterion ensures that our mesh effectively captures the intricate details and nuances of the part's geometry, contributing to the reliability and accuracy of our simulation outcomes.

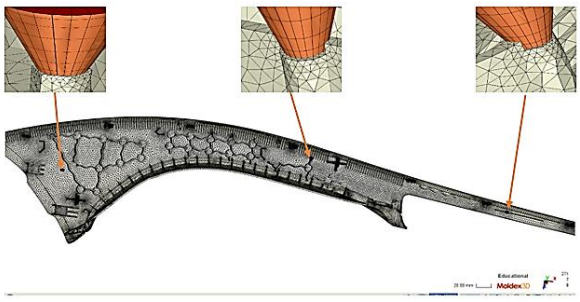

Fig. 6. Meshing of the component carrier side flank

3.3. Material

For the MuCell simulation, the part has been injected with ABS (Acrylonitrile Butadiene Styrene) of the Terluran HH-106 type. This material provides excellent resistance to thermal deformation and impact, along with improved surface quality, making it well-suited for automotive applications.

3.4. Numerical Modelling of the MuCell® Injection Moulding Process

The simulation is conducted using the "Computer-Aided Engineering Mode," wherein parameters are automatically defined based on dimensions, volume, material characteristics, and other relevant factors. The following injection parameters, listed in Table 2, are used:

Table 2. Injection parameters

Injection pressure	155 MPa
Filling time	2.46 sec
Hold and compaction time	0.1 sec
Melting temperature	250 °C
Mould temperature	60 °C

The melting temperature and mould temperature are configured based on the specifications provided in the material data sheet. Foaming parameters are set by default as follows:

- Shot weight control (V/P Switch) by 95% shot weight percentage.
- Initial gas concentration: Amount of gas dosed: 0.5 wt%.

The characteristics of nitrogen are defined as presented in figure 7.

3.5. Results

The flow results are presented in two stages: the V/P transition stage signifies the point, typically a percentage of the total volume (defaulting to 95%), at which the injection moulding machine shifts from

speed control (filling) to pressure control (compaction) during the filling process. Consequently, at the time of the V/P switchover, some areas of the part may remain unfilled, and these regions, which have not been reached by the flow front, are depicted in grey, as illustrated in figure 8. Following the transition, the part is filled at a consistent pressure.

3.5.1. Cell size

During microcellular injection, the expansion of cells plays a crucial role in shaping the final structure of the component. The term "cellular growth" refers to the formation and expansion of microscopic cells within the material matrix. These cells are usually within the size range of 5 to 100 microns. This cellular structure imparts unique properties to the material, such as reduced density and enhanced mechanical characteristics, making it a valuable technique for various applications. The simulation results of bubble growth within the cavity are depicted in figure 9.

Figure 10 illustrates the results depicting the cell diameter concerning its relationship with the distance from the core. Given that the pressure is significantly higher at the injection gates, the cell size is smaller.

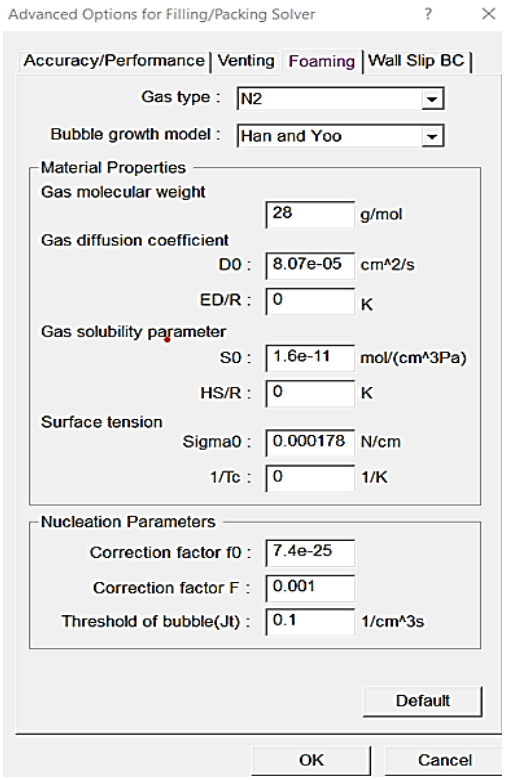

Fig. 7. Properties of N2

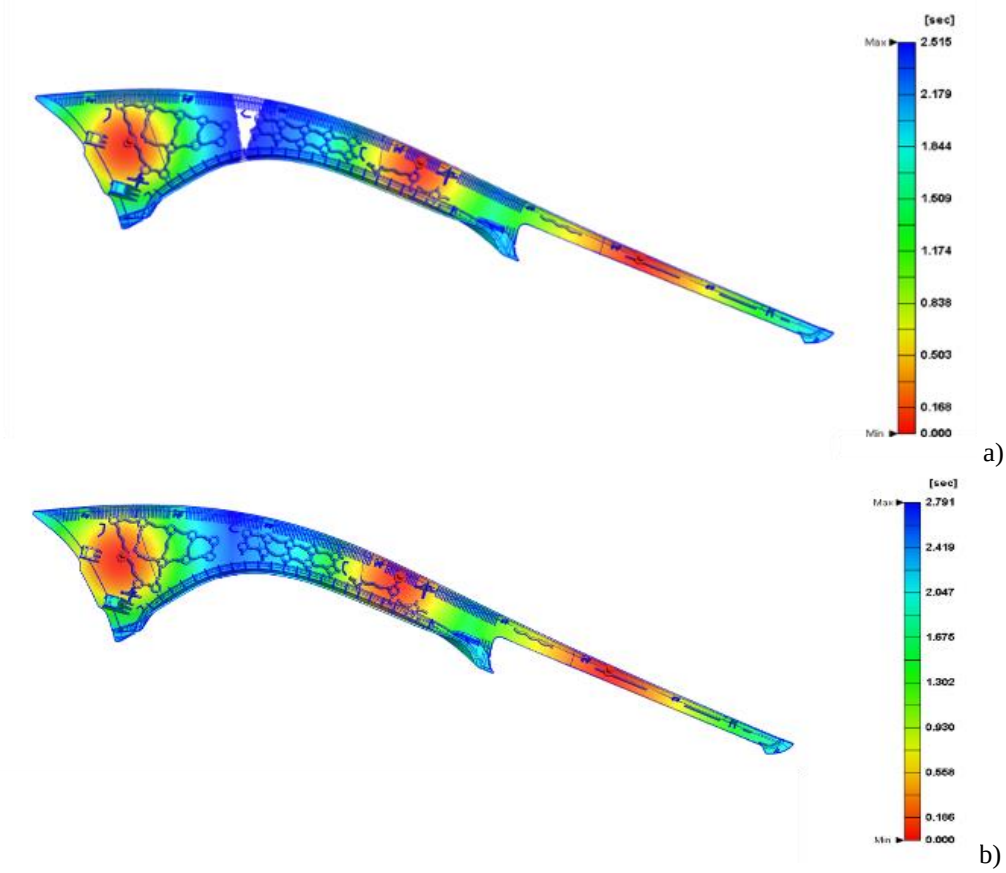

Fig. 8. Filling of the part during V/P switch

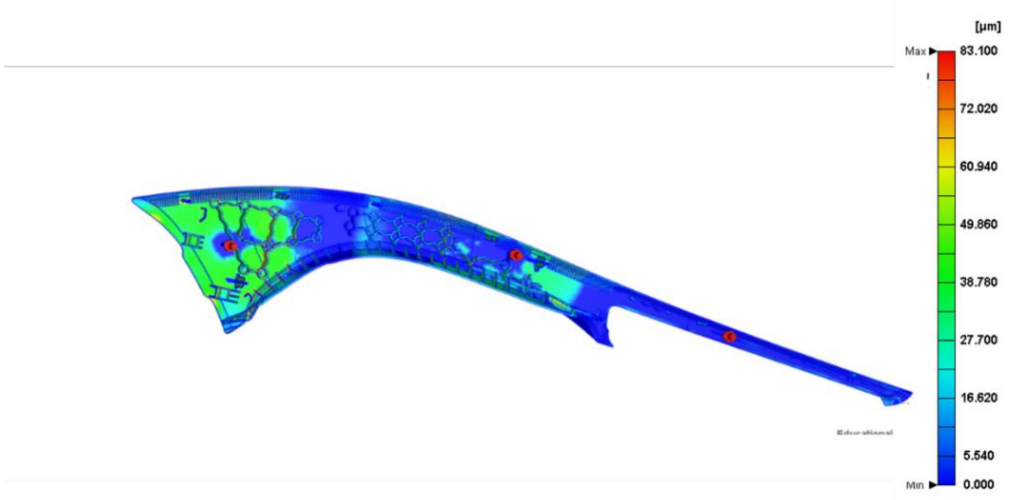

Fig. 9. Cell size

Conversely, as we move farther away from the injection gates, more bubbles tend to form. This phenomenon arises due to the distribution of pressure within the mould during the injection process. Near the injection gates, where the material is forcibly pushed into the mould cavity, the pressure is substantially higher. Consequently, in these regions, the cells that form within the material tend to be smaller in size. Conversely, as we move away from the injection gates and deeper into the mould, the pressure decreases. This reduction in pressure encourages the formation of larger bubbles or voids within the material. This variation in cell size across different regions of the part can have a significant impact on its final properties and characteristics.

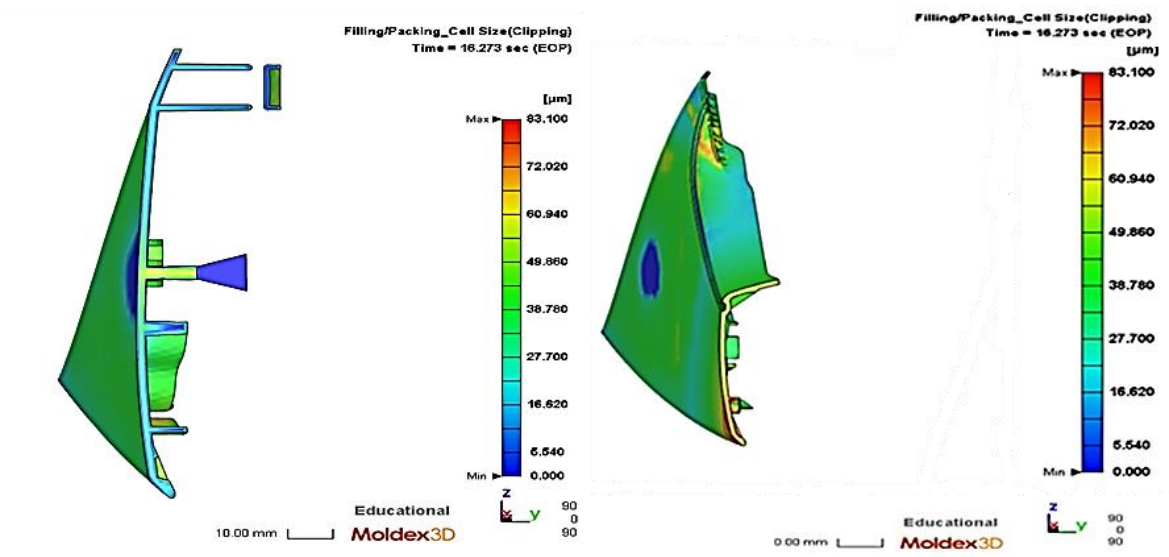

Fig. 10. Size of cells near injection gates, away from injection gates

3.5.2. Cell density

Cellular density refers to the numerical concentration of bubbles within a material. A higher value signifies a greater number of bubbles per unit of volume. Figure 11 shows the simulation results for cell density.

The unit 1/cc (or 1 cm^3) for cell density means that the measurement is expressed in terms of the number of bubbles per cubic centimeter. In this case, the value indicates 65.22 million bubbles in every cubic centimeter of material, which is extremely high. This suggests a very fine, well-distributed foam. Such a high cell density can enhance characteristics like thermal insulation, sound absorption, and the lightweight nature of the material. This can be particularly valuable in applications where weight and thermal efficiency are crucial.

3.5.3. Trapped air

Upon inspection, it becomes evident that numerous air bubbles are present on the functional surfaces of the

part figure 12 (blue points). To mitigate these defects, the incorporation of vents within the mould can serve as an effective solution.

Air entrapment during the injection moulding process can lead to the formation of unwanted bubbles, particularly on the critical surfaces of the part. These bubbles can compromise the part's integrity and functionality. Vents are strategically placed channels or openings in the mould that allow trapped air to escape as the material flows in. This helps in achieving defect-free parts by preventing air from getting trapped within the mould cavity, ensuring a smoother and more reliable injection moulding process.

3.5.4. Welding lines

In this injection process, three injection gates were employed simultaneously, resulting in the convergence of melt fronts at two distinct levels within the mould cavity. This convergence gave rise to the formation of welding lines (Fig. 13).

Weld lines, or weld marks, occur in injection moulding when the molten material flows together after being split and redirected by multiple gates or flow paths. These lines can sometimes weaken the structural integrity of the final part, and their appearance is often considered a cosmetic defect. By understanding the flow patterns and optimizing gate placement, it's possible to minimize or eliminate the formation of these weld lines during the injection moulding process.

3.5.5. Volumetric shrinkage

In the context of injection moulding, volumetric shrinkage represents the reduction in the overall volume of a moulded part as it cools and solidifies after being injected into the mould. This phenomenon typically occurs due to the material's response to changes in pressure, temperature, and volume as it transitions from a molten state to a solid state. The mentioned 2.7% shrinkage is an expected and relatively uniform reduction in the part's size throughout the entire cavity (figure 14), a characteristic often attributed to the presence of microbubbles within the material. These microbubbles help distribute the shrinkage more evenly, leading to a more consistent and controlled final part size.

3.5.6. Sink marks

Sink marks refers to the excess material that can sometimes escape from the mould cavity during the injection moulding process and solidify on the part's surface. This excess material can create imperfections on the final part and requires additional post-processing to remove. In the context of microcellular injection, one advantage is the reduced likelihood of flash occurrence due to the controlled and uniform expansion of the material with the presence of microbubbles. This leads to a part with a smoother and cleaner surface finish, reducing the need for post-processing and enhancing overall part quality (Fig. 15).

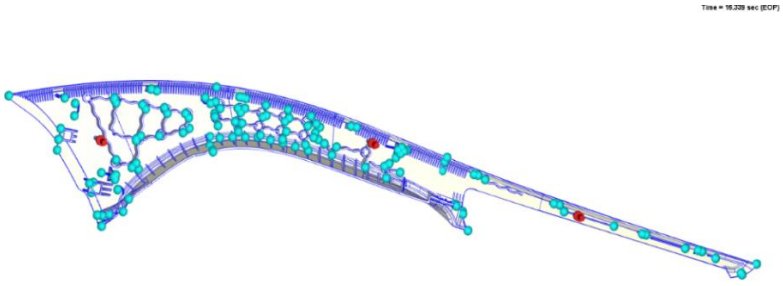

Fig. 11. Cell density within the part

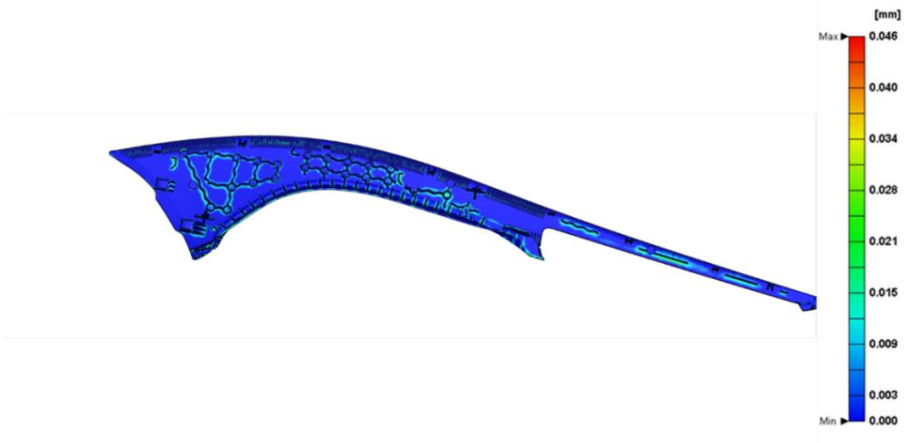

Fig. 12. Trapped air injection defect

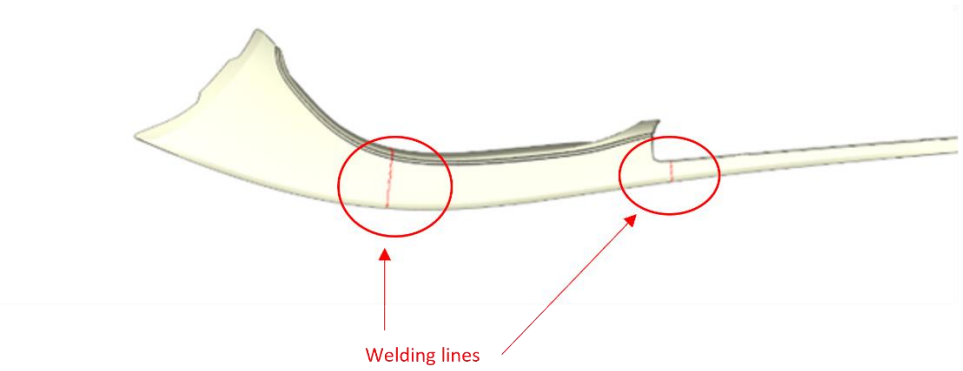

Fig. 13. Welding lines

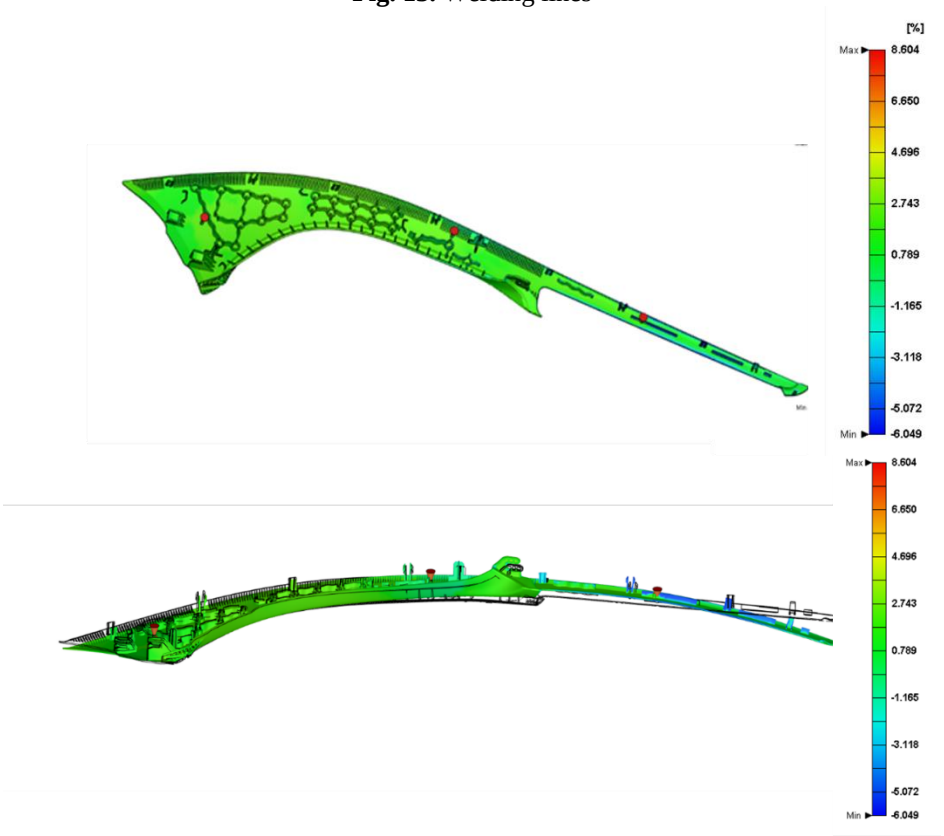

Fig. 14. Volumetric shrinkage of the part

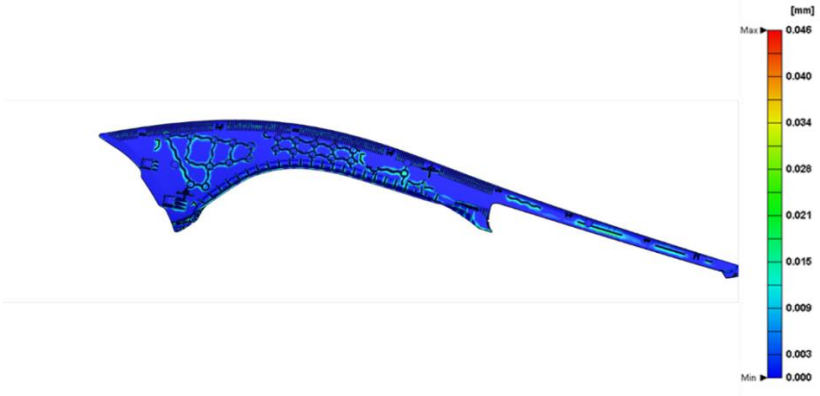

Fig. 15. Sink mark displacement

3.5.7. Deformation

Deformation in injection-moulded parts can occur due to a variety of factors, including material characteristics, processing conditions, and the geometry of the part itself. It involves changes in the shape or dimensions of the part from its intended design. The figures 16 to 18 provide visual representations of the extent of deformation in different directions, with the Y and Z directions being particularly important to understand how the part may deviate from its intended shape. Minimizing deformation is a key goal in injection moulding to ensure that the final parts meet the required dimensional and quality standards.

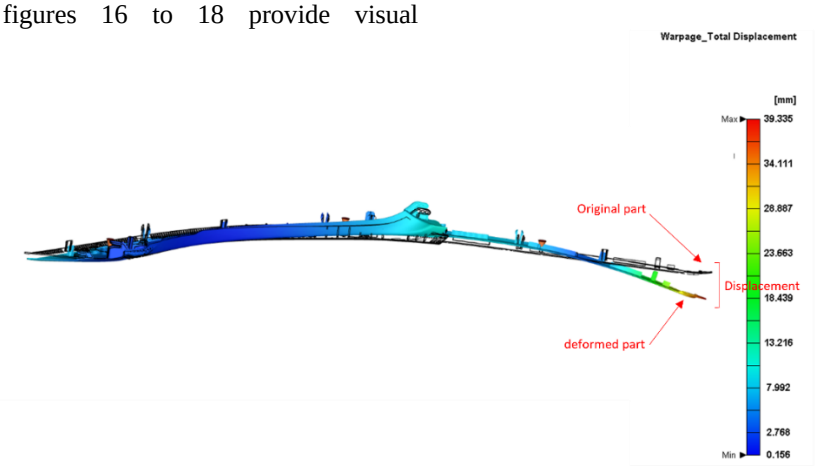

Fig. 16. Total displacement

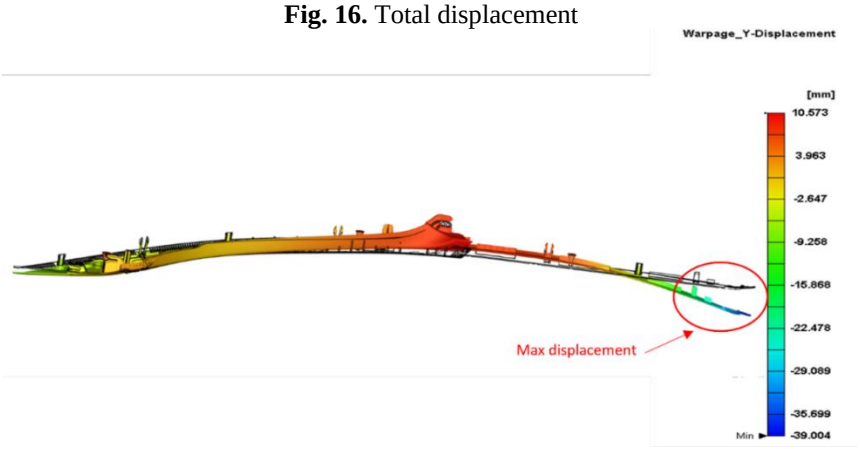

Fig.17. Deformation along the Y axis

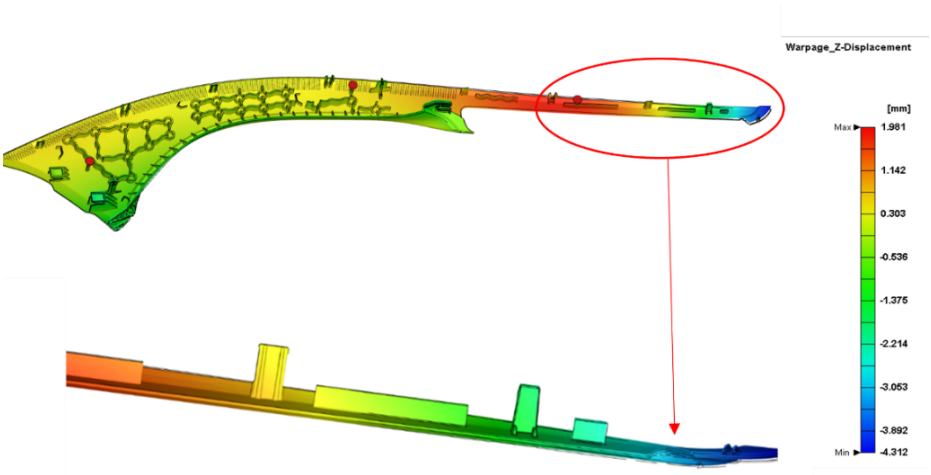

Fig.18. Deformation along the Z axis

3.5.8. Sprue pressure

The use of supercritical fluids in the injection process can alter the flow characteristics of the material being injected. In this context, the reduction in material viscosity leads to an injection pressure requirement equal to 62 MPa (Fig. 19). This graph visually represents how the pressure within the runners or channels changes as the material fills the mould during the injection process.

Understanding these pressure dynamics is essential for optimizing the injection moulding process and achieving consistent and high-quality results.

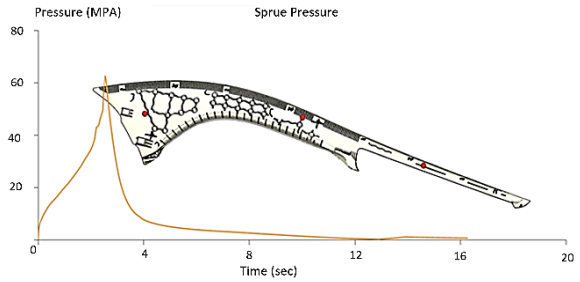

Fig. 19. Sprue pressure

3.5.9. Clamping force

The clamping force initially increases as the molten material is injected into the mould due to the rise in internal pressures that necessitate a stronger hold to prevent the mould from opening (Fig. 20). The clamping force attains its maximum value at the conclusion of the compaction phase, which occurs approximately 2.56 seconds after the beginning of the process. This is since the material has fully filled the cavity, thereby exerting the highest internal pressure against the mould walls. Subsequently, as the molten material cools and solidifies, the internal pressure declines, resulting in a reduction in the requisite clamping force. Consequently, as the material transitions from a molten state to a solid state and begins to shrink, the injection machine can safely decrease the clamping force without compromising the integrity of the mould. This reflects the dynamic changes in pressure and material state throughout the moulding cycle.

Additionally, the reduction of pressure in the runners of the injection moulding process also contributes to a decrease in clamping forces, which in turn gives rise to several benefits. Moreover, this results in enhanced energy efficiency, as less energy is required to operate the moulding machine, thereby reducing operational costs. Moreover, the implementation of diminished clamping forces offers the additional advantage of reducing stress on machine components, which may lead to an extension of the equipment lifespan and a reduction in maintenance needs. Modulating the clamping force in accordance with runner pressure assists in the prevention of over-clamping, which can lead to defects in the manufactured parts and damage to the mould. Furthermore, this approach ensures the maintenance of consistent part quality by minimizing the variations that may arise in the moulding process. However, it is of the utmost importance to maintain an appropriate clamping force, as a force that is insufficient may result in the formation of flash or defects if the mould does not remain securely closed during injection. Therefore, the careful management of pressure and clamping forces is essential for the attainment of optimal moulding results.

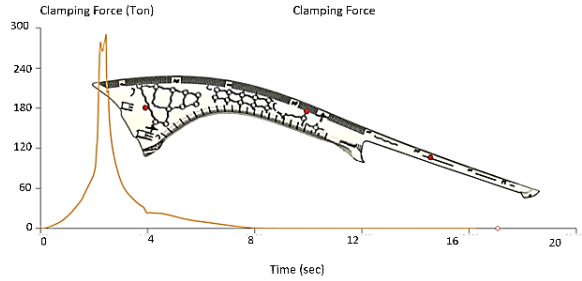

Fig. 20. Clamping force

3.5.10. Part weight

Figure 21 shows the graph of the weight (in g) of the part over the filling time. The total weight of the part is 146.93 g.

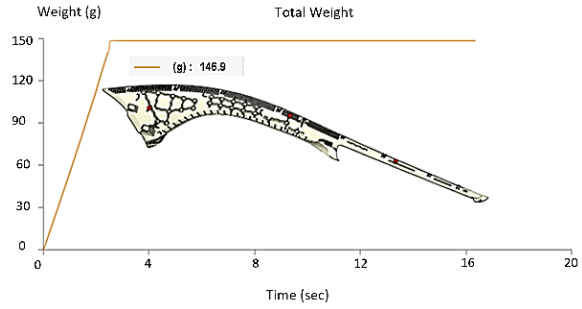

Fig. 21. Part weight

4. COMPARATIVE RHEOLOGICAL STUDY OF CONVENTIONAL INJECTION MOULDING

The primary goal of this project is to conduct a comprehensive analysis comparing MuCell injection with standard injection methods. This analysis is intended to confirm and validate the unique characteristics attributed to microcellular injection technology.

1st iteration

Depending on the part dimensions and material properties, Moldex3D establishes the following default injection parameters (Table 3): The melting

temperature and mould temperature are configured based on the specifications provided in the material data sheet.

Result

During the dynamic injection phase, the flow is incomplete, meaning that the part still requires additional material to fully fill (Fig. 22). Therefore, we move on to the holding phase, which allows us to complete the filling process and compensate for any part shrinkage phenomena (Fig. 23). The error indicates that the filling time is insufficient. Moldex3D provides a second filling time, based on the time taken previously.

Table 3. Injection parameters

Injection pressure	155 MPa
Holding pressure	100 MPa
Filling time	2.46 s
Hold and compaction time	6.31 s
Melting temperature:	250 °C
Mold temperature	60 °C

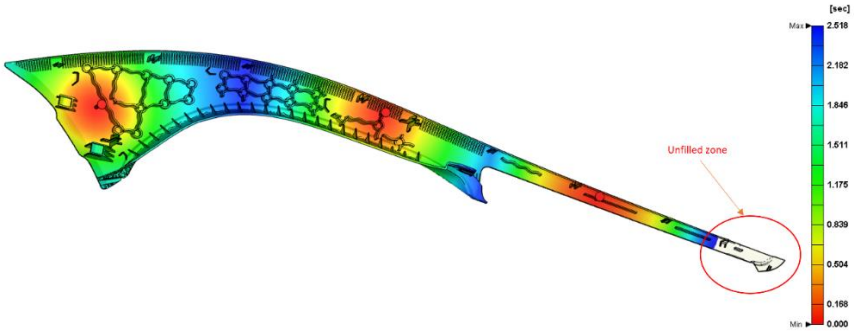

Fig. 22. Material flow during the filling phase

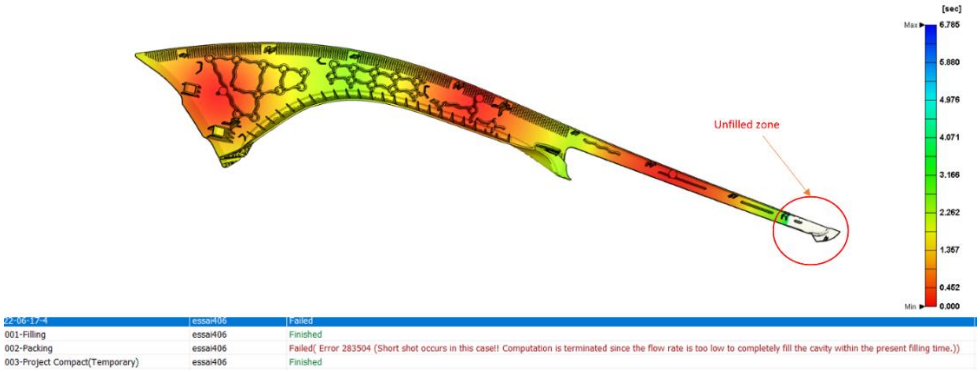

Fig. 23. Holding and compaction phase

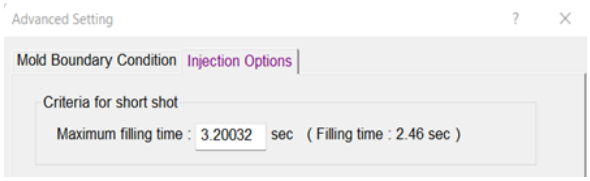

Fig. 24. Calculation of filling time using Moldex3D

2nd iteration

We re-run the study by adjusting the filling time while keeping the other parameters constant (Fig. 25).

Result:

The flow level of the part has improved, but it is still insufficient to achieve complete filling (Fig. 26).

3rd iteration

We use the updated injection parameters as follows in Table 4:

Result:

With the injection conditions set as previously mentioned, we achieve complete and consistent flow as shown in figure 27.

Table 4. Updated injection parameters

Injection pressure	155 MPa
Holding pressure	100 MPa
Filling time	4.16 sec
Holding and compaction time	6.31 sec

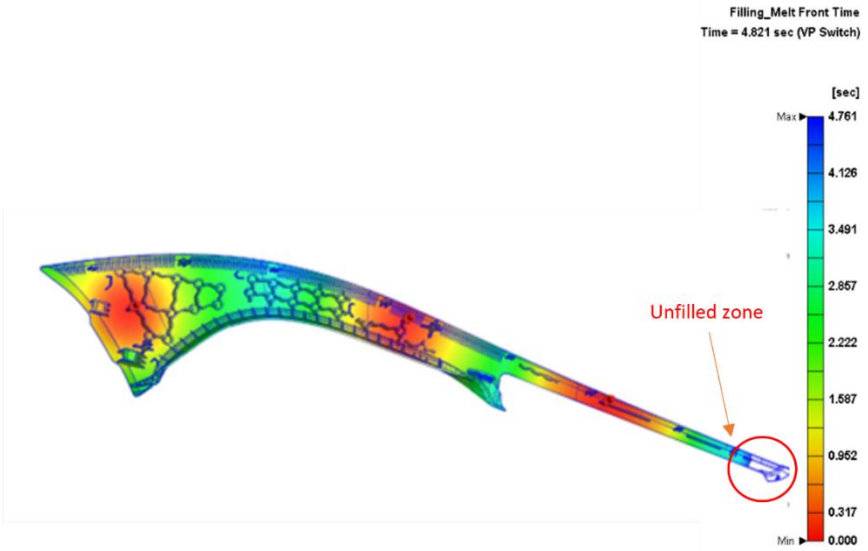

Fig. 25. Filling phase

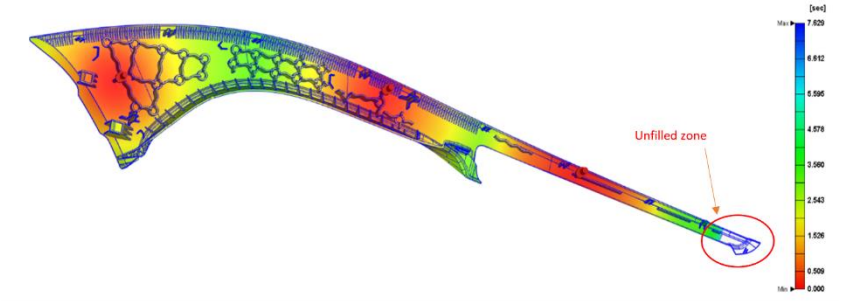

Fig. 26. Holding and compaction stage

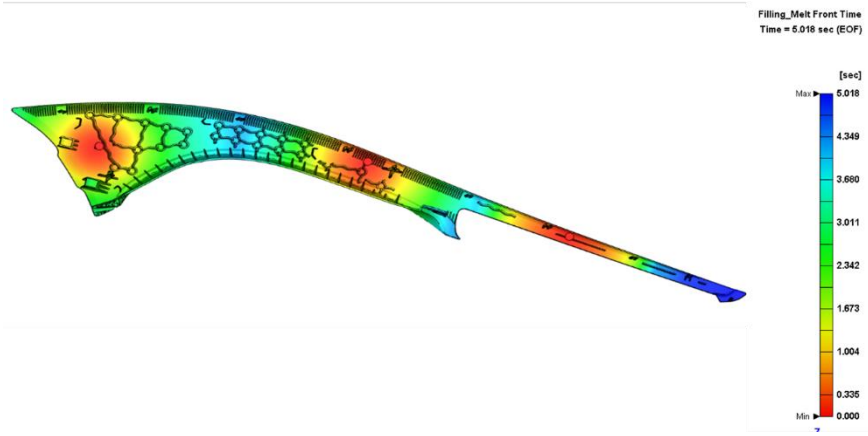

Fig. 27. End of material flow

Welding lines

The quality of moulded parts is significantly influenced by the quality of the welding lines. In comparison to the preceding results for microcellular injection moulding (figure 13), the weld lines in standard injection moulding are more pronounced (figure 28) and appear visually darker. The darker colouration indicates a concentration of material at the junctions, which may indicate potential structural weaknesses in those areas. The darkness of the weld lines is typically associated with higher material density or concentration, which can lead to diminished mechanical properties and compromised structural integrity in these critical junctions. This is a crucial consideration during the design of parts and the optimisation of the moulding process, as the presence and characteristics of welded lines can significantly impact the overall performance and strength of the final product. It is therefore essential to address the formation and quality of weld lines in order to ensure that the moulded parts meet the required specifications for durability and functionality.

Sink mark

In the MuCell injection process, parts indeed exhibit sink marks and shrinkage that are lower compared to those produced by standard injection molding (Fig. 15 and Fig. 29). This is because, in standard injection, factors such as pressure and holding time have a significant impact on the formation of sink marks, primarily due to the material's contraction during cooling. In contrast, in microcellular injection, the expansion of gas cells within the material helps reduce sink marks. As the gas expands, it creates a sort of holding effect that limits the contraction of the material, resulting in fewer deformations and, consequently, fewer sink marks on the finished parts.

Thus, the use of MuCell technology enhances part quality by minimizing defects associated with shrinkage, unlike standard injection molding.

Deformation and volume shrinkage

Based on the above results, it's clear that MuCell injection moulding has the advantage of reducing deformation and shrinkage, as the expansion of the gas eliminates the holding phase and thus largely eliminates residual stresses in the part.

The total deformation of the part in conventional injection moulding is 52.865 mm, as shown in figure 30. Figures 31 and 32 illustrate the simulated deformations along the Y and Z axes, respectively. For instance, the deformation along the Y-axis measures approximately 16.324 mm, while the deformation along the Z-axis is around 3.687 mm. Additionally, figure 33 presents the volumetric shrinkage, revealing the overall reduction in the part's volume as it cools and solidifies.

Clamping force and gate pressure

As the filling process progresses, there is a notable rise in clamping force, peaking at the moment of complete part filling and compacting, which occurs precisely at 4.8 seconds (Fig. 34). Beyond this point, the holding phase primarily functions to compensate for any shrinkage phenomena that may occur, resulting in a gradual reduction in clamping force. In essence, once the part is filled, the primary purpose of the holding phase is to counteract any potential shrinkage, allowing for a controlled and stable moulding process.

This sentence straightforwardly states the requirement for a press with an 800-ton capacity to produce an identical component.

The core pressure remains unchanged, unlike in MuCell injection (Fig. 35).

Part weight

Figure 36 shows the graph of the weight (in g) of the part over the filling time. The total weight of the part injected using the standard injection process is 155.60g.

Comparison of results

Table 5 provides a summary of the simulation process parameters associated with the two technologies and those of the company's experimental MuCell process. The simulation results for the two technologies are presented in Table 6.

Table 5. Simulation process parameters for the two technologies vs the company's MuCell process parameters

	MuCell process parameters	**MuCell**	**Conventional**
Part weight [g]	147	146.93	155.60
Maximum closing force [Ton]	300	290.7 (Fig. 29)	705.2
Injection time [s]	1.97	2.56 (2.46+0.1)	4.16
Hold time [s]	0.1	0.1	6.31
Cycle time [s]	43	39.76 CT=2.56+ 0.1+37.1	47.7 CT=37.23+ 4.16+6.31=47.7

Table 6. MuCell process vs conventional process simulation results

MuCell process parameters	**MuCell**	**Conventional**
Deformation along y [mm]	10.573	16.324
Deformation along z [mm]	1981	3.687
Total deformation (x, y, z) [mm]	39.335	52.865
Shrinkage [%]	8.604	11.33

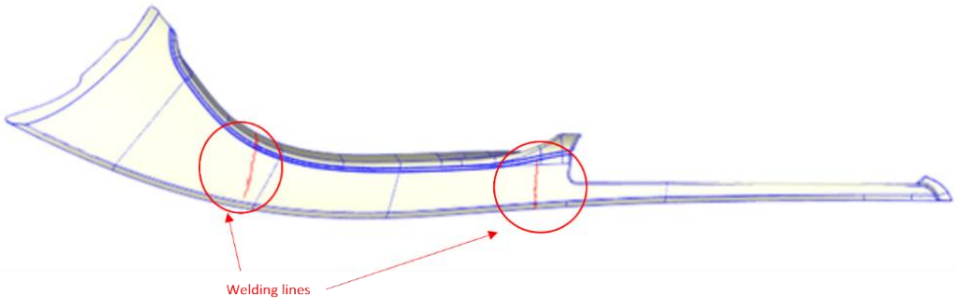

Fig. 28. Welding Lines in Standard Injection

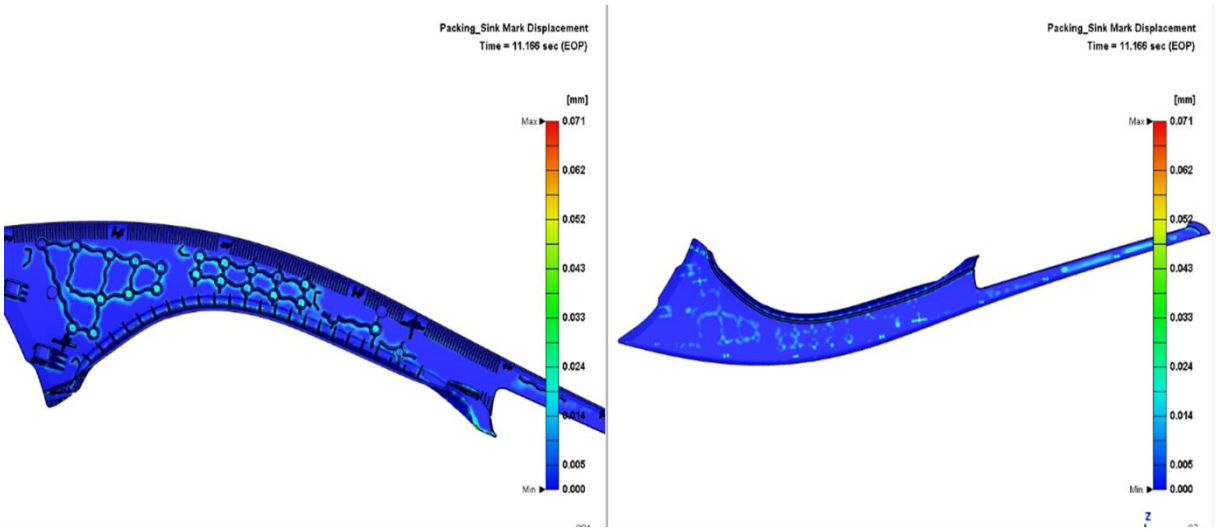

Fig. 29. Sink marks in standard plastic injection

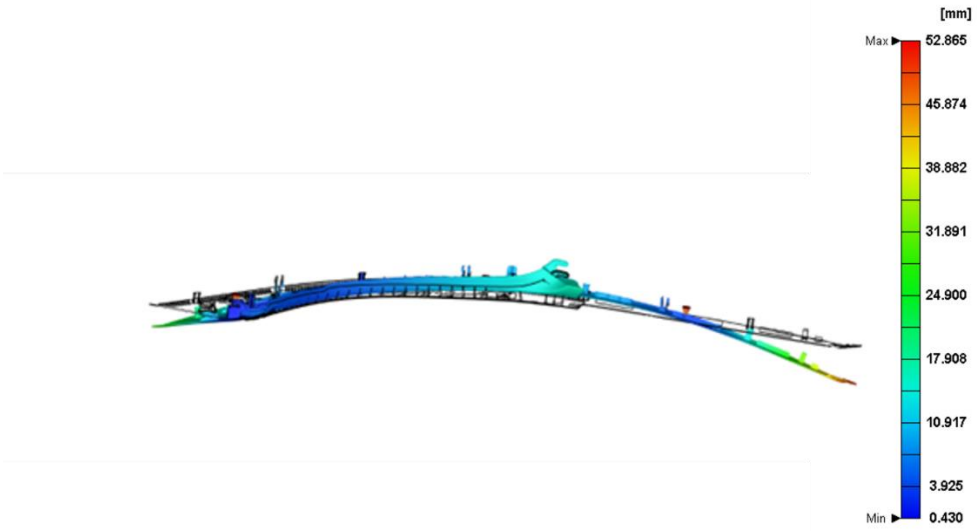

Fig. 30. Total deformation in standard plastic injection

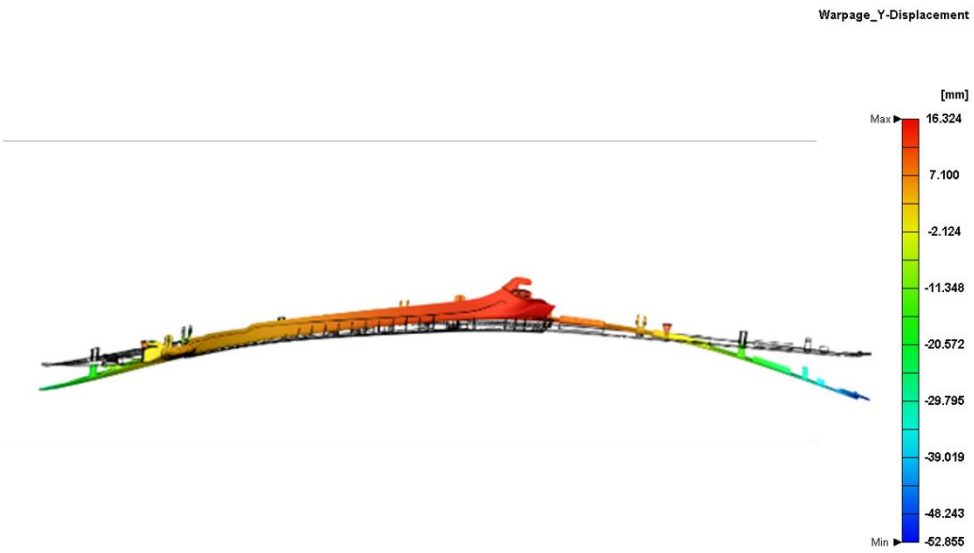

Fig. 31. Deformation along the Y axis in standard plastic injection

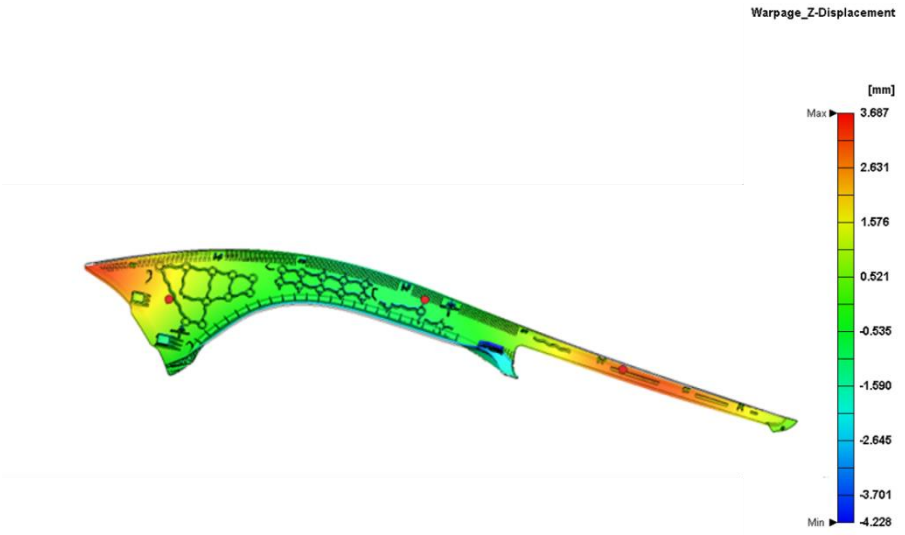

Fig. 32. Deformation along the Z axis in standard plastic injection

Fig. 33. Volume shrinkage in standard plastic injection

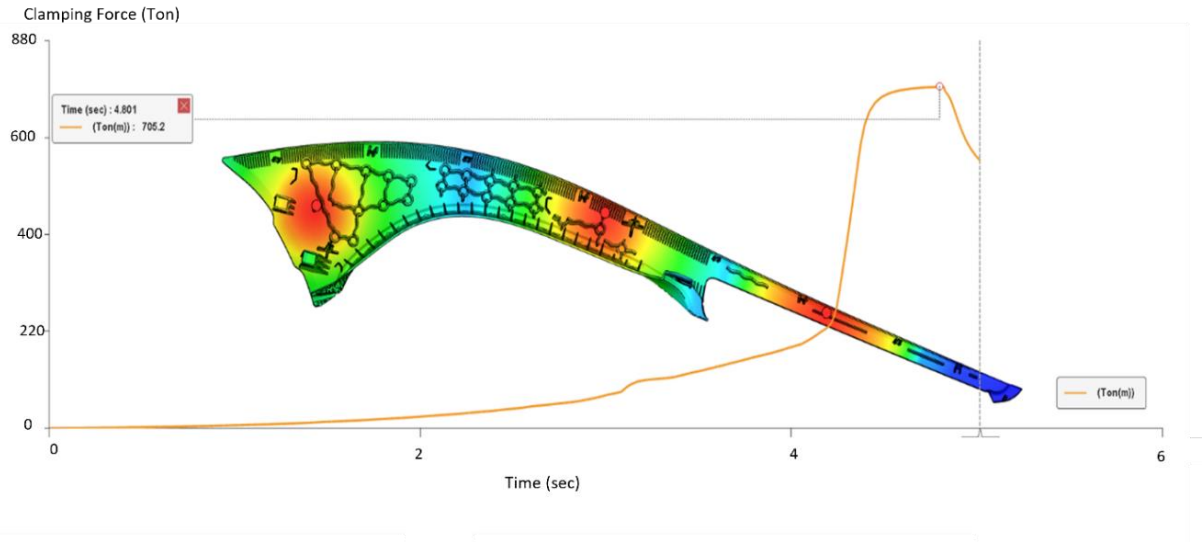

Fig. 34. Clamping force in standard plastic injection

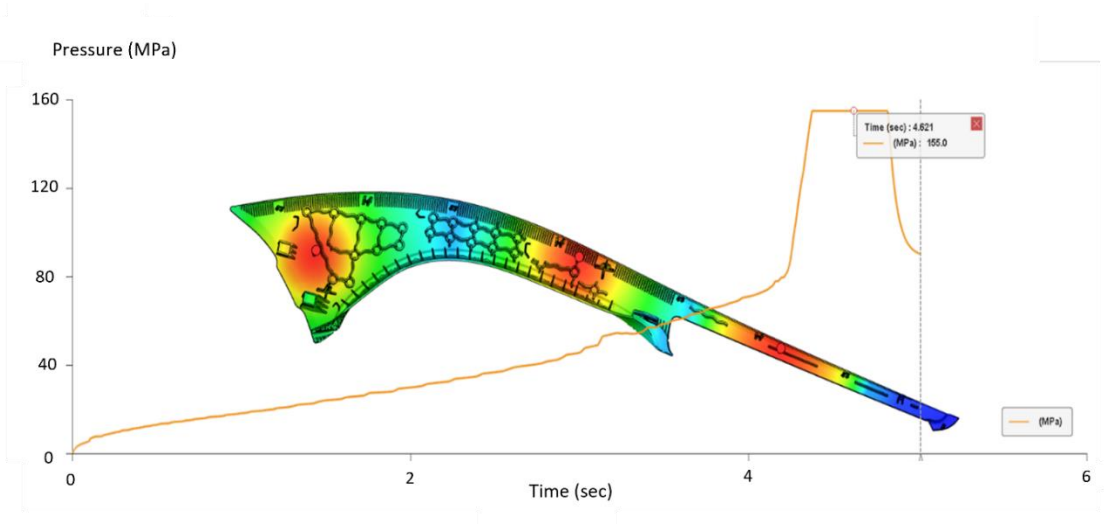

Fig. 35. Core pressure in standard plastic injection

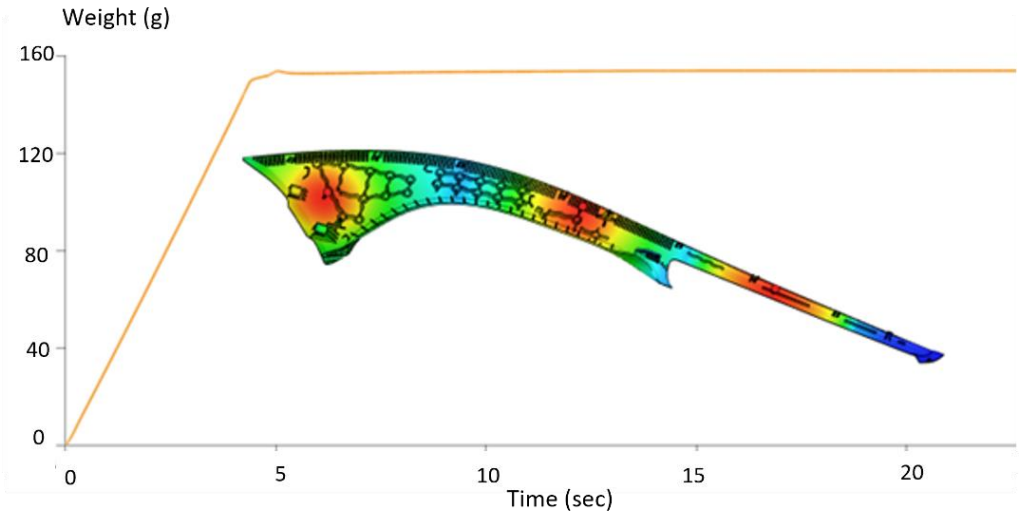

Fig. 36. Part weight in standard plastic injection

From the simulations carried out, we were able to confirm the characteristics of microcellular injection as follows:

- Part weight reduction of 5.5% (density reduction).
- Tonnage reduction from 800 T to 300 T (62.5%).
- 16% cycle time reduction.
- Improved dimensional stability.

In this section, we have established the characteristics of each of the processes to produce the Trager Seitenflanke part, based on the rheological study.

5. CONCLUSIONS

The present technical study of MuCell injection marks a significant step toward a novel microcellular injection technology that has demonstrated technical effectiveness.

To carry out our study successfully, we conducted a technical study by simulating two rheological analyses of the carrier side flank part: the first using the microcellular injection mode and the second using the standard injection mode. The objective of the technical study was to compare the simulation results with those of the current process (MuCell), validating the choice of parameters and affirming the efficacy of the rheological study.

We conclude that MuCell is a relevant injection moulding technique for creating lightweight plastic components with a microcellular internal structure. This technique has enabled us to produce a part, carrier side flank with improved dimensional stability, reduced shrinkage, and less warping compared to the conventional injection-moulded part. Furthermore, microcellular injection has led to a reduction in injection pressure, clamping forces, and cycle time.

Referring to these results, we will develop an economic analysis in future work to assess the profitability of the MuCell process. This analysis will take into account factors such as material costs,

production efficiency, energy consumption, and potential savings that could be achieved through reduced defects and improved part quality. By evaluating these parameters, we aim to provide a comprehensive understanding of the economic benefits that will be associated with the MuCell technology compared to conventional injection moulding.

In conclusion, while MuCell injection moulding presents significant advantages, including weight reduction and material efficiency, it is essential to acknowledge the potential drawbacks associated with this technology. Such drawbacks may include a potential reduction in mechanical properties, such as strength and impact resistance, in addition to challenges pertaining to surface finish and design complexity. Nevertheless, the advantages of MuCell technology frequently outweigh these limitations, rendering it a valuable option for applications where cost savings and reduced weight are of paramount importance. A meticulous assessment of each project will ensure that the most suitable approach is taken, thereby optimizing the advantages of this innovative molding technique.

REFERENCES

[1] **Fernandes C., Pontes A. J., Viana J. C., Gaspar-Cunha A.,** *Modeling and Optimization of the Injection-Molding Process: A Review,* Advances in Polymer Technology, vol. 37, 2018, pp. 429-449.

[2] **Rosato D. V., Rosato M. G.**, *Injection Molding Handbook*, 3rd ed., Springer Science & Business Media, New York, NY, USA, 2012, pp. 1-1460.

[3] **Goodship V., Middleton B., Cherrington R.,** *Injection molding of thermoplastics, in Design and Manufacture of Plastic Components for Multifunctionality*, William Andrew Publishing, Oxford, UK, 2016, pp. 103–170.

[4] **Okolieocha C., Raps D., Subramaniam K., Altstädt V.,** *Microcellular to nanocellular polymer foams: Progress (2004–2015) and future directions—A review,* Eur. Polym. J., 2015, 73: 500–519.

[5] **Xu J.,** *Microcellular Injection Molding*, John Wiley & Sons, Hoboken, NJ, USA, 2011, pp. 1–632.

[6] **Banerjee R., Ray S. S.,** *Foamability and special applications of microcellular thermoplastic polymers: A review on recent advances and future direction*, Macromol. Mater. Eng., 2020, vol. 305, pp. 2000366.

[7] **Štěpek J., Daoust H.,** *Additives for Plastics*, vol. 5, Springer, New York, NY, USA, 1983, Chemical and Physical Blowing Agents, pp. 112–123.

[8] **Iannace S., Park C. B.,** *Biofoams: Science and Applications of Bio-Based Cellular and Porous Materials*, CRC Press, Boca Raton, FL, USA, 2015, pp. 1–466.

[9] **Han C. D., Kim Y. W., Malhotra K. D.,** *A study of foam extrusion using a chemical blowing agent*, Journal of Applied Polymer Science, vol. 20, 1976, pp. 1583–1595.

[10] **Kutz M.,** *Applied Plastics Engineering Handbook: Processing and Materials*, Elsevier Science, Amsterdam, The Netherlands, 2011.

[11] **Wang G., Zhao G. Q., Wang J., Zhang L.,** *Research on formation mechanisms and control of external and Inner bubble morphology in microcellular injection molding,* Polymer Engineering & Science, vol 55, 2015, pp. 807-835.

[12] **Błędzki A. K., Faruk O., Kirschling H., Kuehn J., Jaszkiewicz A.,** *Microcellular polymers and composites*, Polimery, 2006, vol. 51, pp. 697–703.

[13] **Gómez-Monterde J., Hain J., Sanchez-Soto M., Maspoch M. L.,** *Microcellular injection molding: A comparison between MuCell process and the novel micro-foaming technology IQ Foam,* Journal of Materials Processing Technology, vol. 268, 2019, pp. 162–170.

[14] **Elduque D., Clavería I., Fernández Á., Javierre C., Pina C., Santolaria J**., *Analysis of the influence of microcellular injection molding on the environmental impact of an industrial component,* Advances in Mechanical Engineering, vol. 6, 2014, pp. 793269.

[15] **Martini J.,** *The Production and Analysis of Microcellular Foam*, Master's Thesis, Massachusetts Institute of Technology, Cambridge, MA, USA, Jan 1981.

[16] **Doroudiani S., Park C. B., Kortschot M. T.,** *Processing and characterization of microcellular foamed high-density polyethylene/isotactic polypropylene blends*, Polymer Engineering & Science, vol. 38, 1998, pp. 1205-1215.

[17] **Colton J. S., Suh N. P.,** *Nucleation of microcellular foam: Theory and practice,* Polymer Engineering & Science, vol. 27, 1987, pp. 500–503.

[18] **Chong T. H., Ha Y. W., Jeong D. J.,** *Effect of dissolved gas on the viscosity of HIPS in the manufacture of microcellular plastics*, Polymer Engineering & Science, vol. 43, 2003, pp. 1337–1344.

[19] **Siripurapu S., Gay Y. J., Royer J. R., DeSimone J. M., Spontak R. J., Khan S.A.,** *Generation of microcellular foams of PVDF and its blends using supercritical carbon dioxide in a continuous process*, Polymer, vol. 43, 2002, pp. 5511–5520.

[20] **Xu J., Pierick D.,** *Microcellular foam processing in reciprocating-screw injection molding machines*, Journal of Injection Molding Technology, vol. 5, 2001, pp. 152.

[21] **Kharbas H., Nelson P., Yuan M., Gong S., Turng L. S., Spindler R.,** *Effects of nano-fillers and process conditions on the microstructure and mechanical properties of microcellular injection molded polyamide nanocomposites*, Polymer Composites, vol. 24, 2003, pp. 655–671.

[22] **Gong S., Yuan M., Chandra A., Kharbas H., Osorio A., Turng L.,** *Microcellular injection molding*, International Polymer Processing, vol. 20, 2005, pp. 202–214.

[23] **Cardona J.,** *Short Screw Designs for the MuCell Process*, Master's Thesis, University of Massachusetts Lowell, Lowell, MA, USA, Jun 2004.

[24] **Gómez-Monterde J., Sánchez-Soto M., Maspoch M. L.**, *Influence of injection molding parameters on the morphology, mechanical and surface properties of ABS foams,* Advances in Polymer Technology, vol. 37, 2018, pp. 2707–2720.

[25] **Oprea-Kiss A., Kiss I.,** *About the numerous cost and processing advantages of the microcellular foam injection molding process for thermoplastics materials in the automobile industry*, Analecta Technica Szegedinensia, vol. 9, 2015, pp. 6–14.

[26] **Pierick D., Janisch R.**, *Microcellular foam molding technology*, Proceedings of the Blowing Agents 99, Blowing Agent Systems: Formulation and Processing Conference, Manchester, UK, 9–10 December 1999.

[27] **Goel S. K., Beckman E. J.,** *Generation of microcellular polymeric foams using supercritical carbon dioxide. I: Effect of pressure and temperature on nucleation,* Polymer Engineering & Science, vol. 34, 1994, pp. 1137–1147.

[28] **Shaayegan V., Wang C., Costa F., Han S., Park C. B.**, *Effect of the melt compressibility and the pressure drop rate on the cell-nucleation behavior in foam injection molding with mold opening*, European Polymer Journal, vol. 92, 2017, pp. 314–325.

[29] **Wu H., Wintermantel E., Haugen H. J.,** *The effects of mold design on the pore morphology of polymers produced with MuCell® Technology*, Journal of Cellular Plastics, vol. 46, 2010, pp. 519–530.

[30] **Suh N. P.,** *Impact of microcellular plastics on industrial practice and academic research*, Proceedings of the IUPAC Polymer Conference on Mission and Challenges of Polymer Science and Technology, Kyoto, Japan, 2–5 December 2002.

[31] **Colton J. S.,** *The nucleation of microcellular foams in semi-crystalline thermoplastics,* Materials and Manufacturing Processes, vol. 4, 1989, pp. 253–262.

[32] **Colton J. S.,** *Ph.D. Thesis, The Nucleation of Microcellular Thermoplastic Foam*, Massachusetts Institute of Technology, Cambridge, MA, USA, Sep. 1985.

[33] **Colton J., Suh N.,** *The nucleation of microcellular thermoplastic foam with additives: Part I: Theoretical considerations*, Polymer Engineering & Science, vol. 27, 1987, pp. 485–492.

[34] **Colton J., Suh N.,** *The nucleation of microcellular thermoplastic foam with additives: Part II: Experimental results and*

discussion, Polymer Engineering & Science, 1987, 27: 493–499. doi: 10.1002/pen.760270703.
[35] **Colton J., Suh N.,** *The nucleation of microcellular thermoplastic foam: Process model and experimental results*, Materials and Manufacturing Processes, vol. 1, 1986, pp. 341–364.
[36] **Moon Y., Cha S. W., Seo J.-h.,** *Bubble nucleation and growth in microcellular injection molding processes*, Polymer-Plastics Technology and Engineering, vol. 47, 2008, pp. 420–426.
[37] **Dong G., Zhao G., Guan Y., Wang G., Wang X**., *The cell forming process of microcellular injection-molded parts*, Journal of Applied Polymer Science, vol. 131, 2014, pp. 40365.
[38] **Waldman F. A.,** *The Processing of Microcellular Foam*, Master's Thesis, Massachusetts Institute of Technology, Cambridge, MA, USA, Jan 1982.
[39] **Behravesh A., Rajabpour M.,** *Experimental study on the filling stage of the microcellular injection molding process*, Cellular Polymers, vol. 25, 2006, pp. 85–97.
[40] **Ishikawa T., Ohshima M**., *Visual observation and numerical studies of polymer foaming behavior of polypropylene/carbon dioxide system in a core-back injection molding process*, Polymer Engineering & Science, vol. 51, 2011, pp. 1617–1625
[41] **Wang L., Ando M., Kubota M., Ishihara S., Hikima Y., Ohshima M., Sekiguchi T., Sato A., Yano H.,** *Effects of hydrophobic-modified cellulose nanofibers (CNFs) on cell morphology and mechanical properties of high void fraction polypropylene nanocomposite foams*, Composites Part A: Applied Science and Manufacturing, vol. 98, 2017, pp.166–173.
[42] **Reniers G., Paltrinieri N.,** *Dynamic Risk Analysis in the Chemical and Petroleum Industry*, 2016, Chapter 16 - Cost-Benefit Analysis of Safety Measures, 195-205.